a standard temperature-controlled (±0.2 °C) water flow system. Observations at 410 and 535 nm were done on independent kinetic runs. Trial experiments on a stopped-flow system, mixing fresh solutions of oxalacetic acid with acidic solutions of $(H_2O)_5CrCH_2CN^{2+}$, indicate that there are no fast absorbance changes preceding those that could be observed on the Cary 219 instrument.

The CO_2 collection studies were done in all glass apparatus connected to a mercury manometer to monitor the CO_2 evolution. A freshly prepared solution of oxalacetic acid was temperature equilibrated for ~5 min in the reaction vessel, and then a similarly equilibrated solution of $(H_2O)_5CrCH_2CN^{2+}$ was injected from a syringe through a stopcock. The apparatus was evacuated with a water aspirator and then closed, and pressure measurements were started about 1 min after mixing. The reaction vessel was immersed in a water bath on a temperature-regulated (±1 °C) hot plate. The overall pressure change depended on the amount of oxalacetic acid and was typically in the range 80-150 mmHg. The volume of the gas collection system was calibrated by weighing the amount of water required to fill the apparatus.

The ^1H and ^{13}C NMR spectra were recorded on a Bruker AM 300 spectrometer. The ^{13}C chemical shifts were measured relative to 5% dioxane, which has a shift of 67.4 ppm relative to TMS. The ^{13}C chemical shifts (relative to TMS) for various functional groups fall into well-defined regions that are rather independent of the chemical species as follows: CH_3(keto), 26 ppm; CH_3(hydrate), 27 ppm; $C(OH)_2$, 93.6 ppm; CO_2H(keto), 168 ppm; CO_2H(hydrate), 174-178 ppm; CO(keto), 202 ppm; dissolved CO_2 was observed at 124.45 ppm.

Acknowledgment. We acknowledge the financial support of the Natural Sciences and Engineering Research Council of Canada.

Contribution from the Department of Chemistry, University of Minnesota, Minneapolis, Minnesota 55455, and Science Research Laboratory, 3M Central Research Laboratories, St. Paul, Minnesota 55144

Electrochemistry and Infrared Spectroelectrochemistry of $[(\eta^5\text{-}C_5R_5)Fe(CO)_2]_2$ (R = H, Me): Generation and Characterization of $[(\eta^5\text{-}C_5R_5)Fe(CO)_2]_2(PF_6)$ Complexes

John P. Bullock,[†] Michael C. Palazotto,[‡] and Kent R. Mann*,[†]

Received September 6, 1990

The electrochemistry of $[CpFe(CO)_2]_2$ (Cp = η^5-cyclopentadienyl) was reexamined under a variety of conditions. This compound, and the related species $[Cp^*Fe(CO)_2]_2$ (Cp^* = η^5-pentamethylcyclopentadienyl), exhibit irreverisble net two-electron oxidations in CH_3CN/TBAH ($E_{p,a}$ = 0.68 and 0.33 V vs AgCl/Ag, respectively) but undergo two, one-electron oxidations in CH_2Cl_2/TBAH. For $[CpFe(CO)_2]_2$, these occur at 0.68 and 1.28 V, while in the $[Cp^*Fe(CO)_2]_2$ complex they occur at 0.34 and 1.16 V. The first process is quasi-reversible for each compound and generates the corresponding binuclear radical cations. The binuclear radical cations were generated and characterized via UV-vis and infrared spectroelectrochemistry. $[CpFe(CO)_2]_2^+$ exists as a mixture of the cis and trans carbonyl-bridged isomers in solution with ν(CO) at 2023, 2055, and 1934 cm^{-1}. $[Cp^*Fe(CO)_2]_2^+$ exists only as the trans isomer in solution with λ_{max} = 518 nm and ν(CO) at 1987 and 1884 cm^{-1}. The binuclear radical-cation species $[CpFe(CO)_2]_2^+$ has long been invoked as an intermediate in the oxidation chemistry of $[CpFe(CO)_2]_2$ but has never been cleanly generated or characterized prior to this work. EPR spectra were observed for both radical cations. $[CpFe(CO)_2]_2^+$ has $g_\parallel$ = 2.004 and $g_\perp$ = 2.084, while $[Cp^*Fe(CO)_2]_2^+$ has $g_\parallel$ = 1.999 and $g_\perp$ = 2.088. These cations are susceptible to rapid, ligand-induced disproportionation reactions. When the ligand is acetonitrile, the proposed mechanisms of these reactions involve the generation and subsequent decomposition of acetonitrile adducts of the radical cation species, e.g., $\{[CpFe(CO)_2]_2(NCCH_3)\}^+$. For the Cp^* compound, the intermediate is short-lived. Stopped-flow measurements of the reaction of $[Cp^*Fe(CO)_2]_2^+$ with CH_3CN showed that the reaction is first order in $[[Cp^*Fe(CO)_2]_2^+]$ and $[CH_3CN]$ with k = 118 (±2) M^{-1} s^{-1}. Cyclic voltammetry studies detected the Cp-containing intermediate $\{CpFe(CO)_2]_2(NCCH_3)\}^+$. The initially formed decomposition products, in the case of $[CpFe(CO)_2]_2^+$, are the 18-electron cationic species $[CpFe(CO)_2(NCCH_3)]^+$ and the 17-electron radical $CpFe(CO)_2^\cdot$. In subsequent reactions, the latter species generates $[CpFe(CO)_2]_2$ and, to a lesser extent, $CpFe(CO)_2Cl$.

Introduction

The electrochemistry of metal-metal bonds has been an area of active research for several years.[1,2] Among the most frequently studied compounds in this area has been $[CpFe(CO)_2]_2$.[2-7] In 1966, Dessy and co-workers reported that the formal iron-iron bond can be reductively cleaved via a net two-electron process at mercury electrodes.[2] Miholová and Vlcek later studied the reduction process in detail and reported that it occurs via an ECE mechanism involving an initial diffusion-controlled electron transfer.[3] The electrochemical oxidation of $[CpFe(CO)_2]_2$ has also been studied. In 1971, Meyer and co-workers published a report that discussed the electrooxidation of $[CpFe(CO)_2]_2$ in a variety of solvents.[4] It was found that in coordinating solvents, e.g., acetonitrile, the oxidation proceeds by two electrons and yields the monomeric metal-solvent adduct cation (eq 1). In

$$[CpFe(CO)_2]_2 \xrightarrow{CH_3CN} 2[CpFe(CO)_2(NCCH_3)]^+ + 2e^- \quad (1)$$

CH_2Cl_2/TBAH, while the overall oxidation was also reported to proceed by two electrons, it was proposed to proceed via an initially generated one-electron oxidized species; no direct observation of this intermediate was reported however. Later, the electrochemistry of this compound was reexamined, also in CH_2Cl_2/TBAH, and was found to exhibit a reversible one-electron oxidation (E° = +0.67 V vs SCE), followed by a second, irreversible oxidation peak at 1.21 V.[7] An attempted bulk electrolysis of the dimer between the two oxidation processes, however, resulted in the removal of two electrons per dimer and generation of a species assigned as $CpFe(CO)_2(PF_6)$.

* To whom correspondence should be addressed.
[†] University of Minnesota.
[‡] 3M Central Research Laboratories.

(1) For leading articles in this field, see: (a) Dessy, R. E.; Stary, F. E.; King, R. B.; Waldrop, M. *J. Am. Chem. Soc.* **1966**, *88*, 471. (b) Dessy, R. E.; Weissman, P. M.; Pohl, R. L. *J. Am. Chem. Soc.* **1966**, *88*, 5117. (c) Denisovich, L. I.; Ioganson, A. A.; Gubin, S. P.; Kolobova, N. E.; Anisimov, K. N. *Bull. Acad. Sci. USSR, Div. Chem. Sci. (Engl. Transl.)* **1969**, *18*, 218. (d) Pickett, C. J.; Pletcher, D. *J. Chem. Soc., Dalton Trans.* **1975**, 879. (e) Meyer, T. J. *Prog. Inorg. Chem.* **1975**, *19*, 1. (f) Lemoine, P.; Giraudeau, A.; Gross, M. *Electrochim. Acta* **1976**, *21*, 1. (g) Lemoine, P.; Gross, M. *J. Organomet. Chem.* **1977**, *133*, 193. (h) de Montauzon, D.; Poilblanc, R.; Lemoine, P.; Gross, M. *Electrochim. Acta* **1978**, *23*, 1247. (i) Madach, T.; Vahrenkamp, H. *Z. Naturforsch., B: Anorg. Chem., Org. Chem.* **1979**, *34B*, 573. (j) Connelly, N. G.; Geiger, W. E. *Adv. Organomet. Chem.* **1984**, *23*, 1. (k) Lacombe, D. A.; Anderson, J. E.; Kadish, K. M. *Inorg. Chem.* **1986**, *25*, 2074. (l) Jaitner, P.; Winder, W. *Inorg. Chim. Acta* **1987**, *128*, L17.
(2) Dessy, R. E.; Weissman, P. M.; Pohl, R. L. *J. Am. Chem. Soc.* **1966**, *88*, 5117.
(3) Miholová, D.; Vlcek, A. A. *Inorg. Chim. Acta* **1980**, *41*, 119.
(4) Ferguson, J. A.; Meyer, T. J. *Inorg. Chem.* **1971**, *10*, 1025.
(5) Moran, M.; Cuadrado, I.; Losada, J. *Inorg. Chim. Acta* **1986**, *118*, 25.
(6) Davies, S. G.; Simpson, S. J.; Parker, V. D. *J. Chem. Soc., Chem. Commun.* **1984**, 352.
(7) Legzdins, P.; Wassink, B. *Organometallics* **1984**, *3*, 1811.

0020-1669/91/1330-1284$02.50/0

The electrochemistry of a similar compound, the bis(diphenylphosphino)ethane-substituted species, $[CpFe(CO)]_2(\mu\text{-dppe})$, exhibits a quasi-reversible one-electron oxidation in a variety of solvents, including CH_3CN, to yield a radical cation that retains the dimeric structure of the parent compound.[8,9] The radical species, while stable in methylene chloride for extended periods, disproportionates relatively slowly in acetonitrile ($t_{1/2} \sim 30$ min at ambient temperature). The formal bond order of the metal–metal interaction in the oxidized species is one-half.

This paper describes our observations concerning the electrochemistry of $[CpFe(CO)_2]_2$ and the related species $[Cp^*Fe(CO)_2]_2$ (Cp^* = pentamethylcyclopentadienyl). We have found that each of these compounds gives rise to binuclear radical cations analogous to $\{[CpFe(CO)]_2(\mu\text{-dppe})\}^+$[8-10] via quasi-reversible one-electron oxidations in CH_2Cl_2/TBAH. The radical-cation species $[CpFe(CO)_2]_2^+$ has long been purported to be the initial product of both the electrochemical[4,7] and chemical[11] oxidation of $[CpFe(CO)_2]_2$, but to date no spectral characterization of this complex had been obtained. Through the use of infrared spectroelectrochemistry, we have been able to generate and characterize the one-electron oxidized products for each of the above species. Moreover, we propose a mechanistic scheme that explains the electrochemical oxidation of these compounds under a variety of conditions. In all cases, we believe that the observed chemistry can be explained by the generation of an intermediate binuclear radical and its subsequent reactivity toward the solvent or electrolyte.

Experimental Section

Syntheses. $[CpFe(CO)_2]_2$ was purchased from Pressure Chemicals and used without further purification. $[Cp^*Fe(CO)_2]_2$ was purchased from Strem Chemicals and was used as received.

Electrochemical Measurements. All electrochemical experiments were performed with a BAS 100 electrochemical analyzer unless otherwise noted.

Cyclic voltammetry (CV) was performed at ambient temperature (25 °C) with a normal three-electrode configuration consisting of a highly polished glassy-carbon-disk working electrode (A = 0.07 cm^2) and a AgCl/Ag reference electrode containing 1.0 M KCl. The working compartment of the electrochemical cell was separated from the reference compartment by a modified Luggin capillary. All three compartments contained a 0.1 M solution of the supporting electrolyte.

The dichloromethane and supporting electrolyte, tetrabutylammonium hexafluorophosphate (TBAH) (Southwestern Analytical Chem., Inc.), were used without further purification. Acetonitrile was distilled over P_2O_5 under dinitrogen prior to use.

Electrolyte solutions of methylene chloride was prepared and stored over 80–200-mesh activated alumina and activated 4-Å molecular sieves prior to use in the experiments. Electrolyte solutions of acetonitrile were prepared immediately prior to use by adding electrolyte (dried at 80 °C) to freshly distilled solvent. In all cases working solutions were prepared by recording background cyclic voltammograms of the electrolyte solution before addition of the complex. The working compartment of the cell was bubbled with solvent-saturated argon to deaerate the solution.

Potentials are reported vs aqueous AgCl/Ag and are not corrected for the junction potential. The standard current convention is used (anodic currents are negative). To allow future corrections and the correlation of these data with those of other workers, we have measured the $E°$ for the ferrocenium/ferrocene couple[12] under conditions identical with those used for the compounds under study. In CH_2Cl_2/TBAH, $E°$ = 0.460 V; in acetonitrile/TBAH, $E°$ = 0.408 V. No iR compensation was used.[13]

Due to extreme water sensitivity of the electrogenerated radical cations, all electrolyte solutions upon which large scale (25–35 mL) bulk electrolyses were performed were dried immediately before use by passage down a column of activated alumina (Fisher, neutral activity 1, 80–200 mesh; activated at 300 °C), before addition of the compound under study. Bulk electrolyses were performed with a platinum mesh electrode. All bulk electrolyses were performed in the dark in order to prevent photolytic side reactions. Bulk solutions of the radical dimer species were used for kinetic studies and ESR measurements.

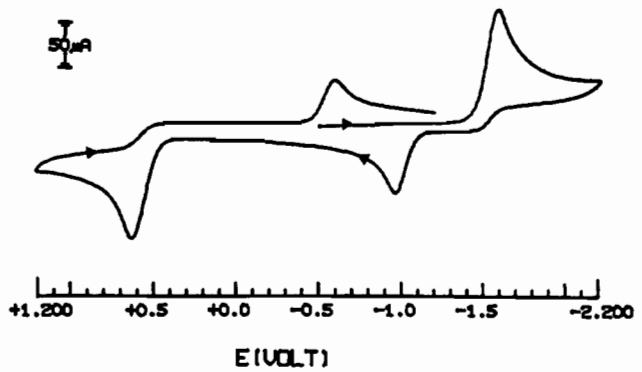

Figure 1. Cyclic voltammogram of a 1.57 mM solution of $[CpFe(CO)_2]_2$ in CH_3CN/TBAH (scan rate = 250 mV/s). The scan was initiated in the negative direction.

Spectroelectrochemical Experiments. Infrared spectral changes accompanying thin-layer bulk electrolyses were measured by using a flow-through spectroelectrochemical thin-layer cell, as described previously.[14] Infrared data were collected with a Mattson Sirius 100 spectrometer. All IR data were corrected for a stray light error (13%) that originates from the inadvertant collection of light reflected off the front face of the CaF_2 plate of the spectroelectrochemical cell. Bulk electrolyses were controlled by an Electrosynthesis Co. (ESC) 410 potentiostatic controller and an ESC 420-A accessory power unit.

EPR Measurements. X-Band EPR spectra were recorded on a Bruker Model ESP 300 spectrometer equipped with a Bruker ER-4111-VT nitrogen-flow temperature controller. All measurements were obtained at −170 °C. Quartz tubes were used in all experiments. The magnetic field was calibrated with the 2,2-diphenyl-1-picrylhydrazyl hydrate free radical (DPPH) as an external standard (g = 2.0037).[15]

Kinetic Studies. UV–vis stopped-flow kinetic studies were performed by using a Tritech Dynamic Instruments Model SR1A stopped-flow apparatus. Light from a quartz tungsten halogen source passed through the apparatus and was detected by a Tracor-Northern TN-6500 rapid-scan spectrometer. Absorbance measurements were integrated over a 10-nm range (515–525 nm) to enhance the signal-to-noise ratio. All experiments were performed under pseudo-first-order conditions in acetonitrile. In routine handling and transfer, solutions of electrogenerated $[Cp^*Fe(CO)_2]_2^+$ were protected from room light due to the photosensitivity of this species. Acetonitrile solutions were prepared by adding the desired amount of a stock CH_3CN/CH_2Cl_2 solution to CH_2Cl_2/TBAH in order to obtain a given acetonitrile concentration. All solutions were degassed prior to use in the experiments.

Results and Discussion

Electrochemistry of $[CpFe(CO)_2]_2$ in CH_3CN/TBAH. Figure 1 shows the cyclic voltammogram of $[CpFe(CO)_2]_2$ in CH_3CN/TBAH. This compound undergoes two bulk redox processes under these conditions: a net two-electron reduction at −1.66 V vs Ag/AgCl and a net two-electron oxidation +0.55 V. Both processes involve cleavage of the formal iron–iron bond[16-19] to yield monomeric ions (eqs 1 and 2). These results are in good agreement with the observations of other workers.[2-7]

$$[CpFe(CO)_2]_2 + 2e^- \rightarrow 2[CpFe(CO)_2]^- \qquad (2)$$

Each bulk process is coupled to an additional peak in the cyclic voltammogram. The reduction peak is coupled to an anodic process at −1.01 V; this peak is assigned to the net one-electron

(8) Ferguson, J. A.; Meyer, T. J. *Inorg. Chem.* **1972**, *11*, 631.
(9) Ferguson, J. A.; Meyer, T. J. *Inorg. Chem.* **1971**, *10*, 1544.
(10) Haines, R. J.; Du Preez, A. L. *Inorg. Chem.* **1972**, *11*, 330.
(11) Braddock, J. N.; Meyer, T. J. *Inorg. Chem.* **1973**, *12*, 723.
(12) Koepp, H. M.; Wendt, H.; Strehlow, H. *Z. Z. Elektrochem.* **1960**, *64*, 483.
(13) Gagne, R. R.; Koval, C. A.; Lisensky, G. C. *Inorg. Chem.* **1980**, *19*, 2854.
(14) Bullock, J. P.; Mann, K. R. *Inorg. Chem.* **1989**, *28*, 4006.
(15) Drago, R. S. *Physical Methods in Chemistry*; Saunders: Philadelphia, PA, 1977; p 324.
(16) Theoretical[17,18] and experimental[19] considerations imply that there is little direct metal–metal bonding in this species. We use the term "iron–iron bond" throughout this work with this understanding. We do so because the oxidation and reduction chemistry of $[CpFe(CO)_2]_2$, which exhibits extensive parallels with other compounds featuring metal–metal bonds, e.g., $Mn_2(CO)_{10}$, $[CpMo(CO)_3]_2$, etc, is most readily interpreted by invoking this type of bonding.
(17) Benard, M. *Inorg. Chem.* **1979**, *18*, 2782.
(18) Jemmis, E. D.; Pinhas, A. R.; Hoffman, R. *J. Am. Chem. Soc.* **1980**, *102*, 2576.
(19) Mitschler, A.; Rees, B.; Lehmann, M. S. *J. Am. Chem. Soc.* **1978**, *100*, 3390.

oxidation of $[CpFe(CO)_2]^-$, which regenerates the parent dimer (eq 3). The final product of the bulk oxidation, $[CpFe(CO)_2(NCCH_3)]^+$, undergoes a net one-electron reduction at −0.64 V; this process also regenerates the neutral parent dimer (eq 4).[4]

$$2[CpFe(CO)_2]^- \rightarrow [CpFe(CO)_2]_2 + 2e^- \quad (3)$$

$$2[CpFe(CO)_2(NCCH_3)]^+ + 2e^- \rightarrow [CpFe(CO)_2]_2 + 2CH_3CN \quad (4)$$

These data are similar to those obtained by Kadish and coworkers for the isoelectronic species $[CpMo(CO)_3]_2$, which also shows two bulk and two coupled voltammetry peaks; these were assigned to processes analogous to those described above for the iron system.[20] On the basis of the width of the oxidation peak of the molybdenum compound ($|E_p - E_{p/2}| = 62$ mV in CH_3CN and 60 mV in CH_2Cl_2) and other considerations, an ECE mechanism was proposed for this process. This mechanism is briefly described below. The first step in the process, which is the rate-determining step, is an electron transfer to the electrode to generate an intermediate species, a binuclear radical cation, $[CpMo(CO)_3]_2^+$. No direct evidence for the generation of this intermediate was observed however. The binuclear cation then decomposes via heterolytic bond cleavage to yield the 16-electron fragment $[CpMo(CO)_3]^+$ and the 17-electron radical species $CpMo(CO)_3^\bullet$. The final step in the mechanism is a one-electron oxidation of the radical.

The width of the oxidation peak of $[CpFe(CO)_2]_2$ in acetonitrile ($|E_p - E_{p/2}| = 108$ mV, measured at 100 mV/s) is also much larger than the 30 mV expected for a two-electron process.[21] Therefore, the net two-electron oxidation of the iron dimer probably also occurs via an ECE mechanism, such as that proposed for the molybdenum compound above, or an EEC mechanism, in which the second-electron is transferred to the electrode prior to cleavage of the dimer. Additional support for an ECE or EEC mechanism comes from electrochemical and spectroscopic evidence for the generation of $[CpFe(CO)_2]_2^+$, which is the iron analogue of the proposed intermediate in the ECE oxidation mechanism of $[CpMo(CO)_3]_2$; of the two general mechanistic possibilities mentioned above, we strongly favor an ECE-type mechanism. In the absence of nucleophiles, the iron dimer radical is stable toward direct oxidation at the electrode at the bulk oxidation potential; this observation, and other experimental data discussed later, strongly suggest that an EEC mechanism for the oxidation of $[CpFe(CO)_2]_2$ in acetonitrile is unlikely. On the other hand, an ECE mechanism is consistent with the observed reactivity of the radical cation; this species is unstable toward rapid disproportionation in the presence of nucleophiles; thus, it is only observable via the oxidation of $[CpFe(CO)_2]_2$ in weakly coordinating solvent/electrolyte combinations.

Electrochemistry of $[CpFe(CO)_2]_2$ in CH_2Cl_2/TBAH. The electrochemistry of the molybdenum and iron systems are very similar in acetonitrile, but they show marked differences in noncoordinating solvent/electrolyte combinations. While $[CpMo(CO)_3]_2$ exhibits irreversible net two-electron oxidations in coordinating *and* noncoordinating media, $[CpFe(CO)_2]_2$ shows two one-electron oxidations in CH_2Cl_2/TBAH, a noncoordinating solvent/electrolyte. Figure 2 shows the cyclic voltammogram of $[CpFe(CO)_2]_2$ under these conditions. The first anodic process is quasi-reversible ($E_{1/2} = 0.68$ V vs Ag/AgCl; $i_c/i_a = 0.94$; $E_a - E_c = 190$ mV), but the second oxidation process is irreversible ($E_a = 1.28$ V). Note that the peak separation for the first process is larger than expected for a Nernstian couple. This is attributed to a change in the geometry of the complex upon oxidation (vide infra). The two larger reduction peaks coupled to the second oxidation process have been assigned and are discussed below. While these data contrast with the initial report of the cyclic voltammetric behavior of $[CpFe(CO)_2]_2$ in CH_2Cl_2/TBAH, which indicated an irreversible net two-electron oxidation,[4] they are in agreement with those reported in 1984 by Legzdins and Wassink.[7] In the latter work, the first process was assigned as the oxidation of the parent to the dimer radical ction $[CpFe(CO)_2]_2^+$, whereas the second oxidation was assigned to the direct oxidation of the radical species, to yield 2 equiv of $[CpFe(CO)_2]^+$. Their attempts to electrochemically generate a bulk solution of the one-electron oxidized species were unsuccessful but instead yielded a net two-electron oxidation to give $CpFe(CO)_2(PF_6)$.[22]

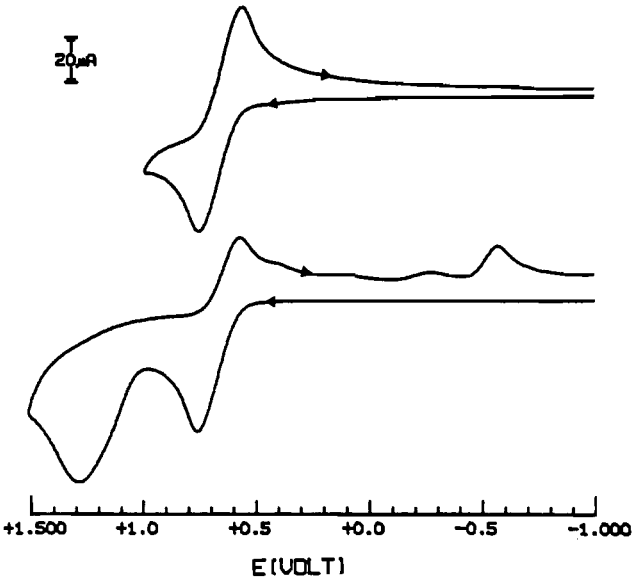

Figure 2. Cyclic voltammogram of a 1.77 mM solution of $[CpFe(CO)_2]_2$ in CH_2Cl_2/TBAH (scan rate = 250 mV/s). The scan was initiated in the positive direction. The sweep direction of the top scan was reversed prior to the second oxidation process to illustrate the reversibility of the first couple.

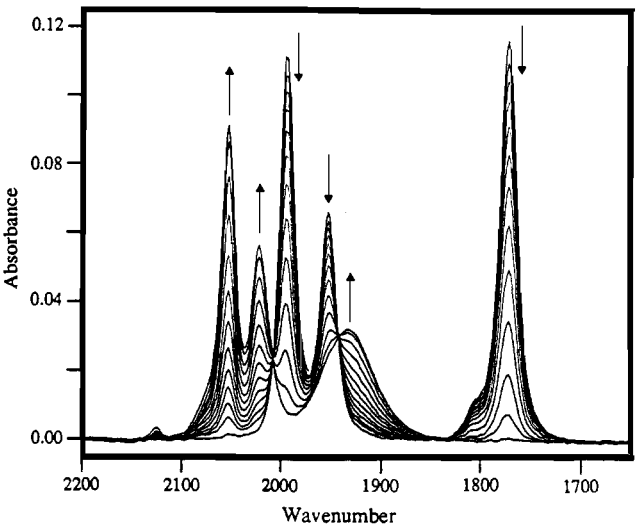

Figure 3. Infrared spectral changes observed upon oxidation of a solution of $[CpFe(CO)_2]_2$ in CH_2Cl_2/TBAH at +1.10 V vs the Pt pseudoreference electrode in the thin-layer spectroelectrochemical cell. The peaks due to the parent dimer, at 1773, 1955, and 1995 cm^{-1}, decrease in intensity as the concentration of the radical-cation dimer, $[CpFe(CO)_2]_2^+$ (ν_{CO} 1934, 2023, and 2055 cm^{-1}), increases during the electrolysis.

(20) Kadish, K. M.; Lacombe, D. A.; Anderson, J. E. *Inorg. Chem.* **1986**, *25*, 2246.

(21) The breadth of the oxidation peak for $[CpFe(CO)_2]_2$ is significantly larger than that which would be expected for a reversible electron-transfer process; this may be indicative of a kinetic barrier to the initial electron transfer; i.e., the first electron transfer may not be a completely reversible process. See: (a) Nicholson, R. S.; Shain, I. *Anal. Chem.* **1964**, *36*, 706. (b) Nicholson, R. S.; Shain, I. *Anal. Chem.* **1965**, *37*, 178.

(22) We believe this assignment is mistaken and that the actual product of the bulk electrolysis was $[CpFe(CO)_2(OH_2)](PF_6)$. Evidence for this comes from a bulk electrolysis of the parent dimer in CH_2Cl_2/TBAH in the presence of excess water; the product of this oxidation had carbonyl peaks (ν_{CO} 2076, 2030 cm^{-1}) that exactly matched those assigned to $[CpFe(CO)_2](PF_6)$.

We have applied infrared spectroelectrochemical techniques to generate and characterize solutions of the one-electron oxidized product of $[CpFe(CO)_2]_2$. Figure 3 shows the infrared spectral changes that accompany the oxidation of this compound in the thin-layer cell at a potential between the two oxidation processes. The carbonyl peaks due to the parent, at 1773, 1955, and 1995 cm^{-1}, all decrease in intensity as those due to the one-electron oxidized compound $[CpFe(CO)_2]_2(PF_6)$ grow in isosbestically at 1934, 2023, and 2055 cm^{-1}, indicating a relatively clean conversion. A small peak observed at 2126 cm^{-1} is due to a small amount of $[CpFe(CO)_3](PF_6)$,[23] which is a decomposition product of the radical cation.[24] We assign the infrared spectrum of the radical in a manner similar to that of the parent, which shows two terminal carbonyl peaks, due to the presence of the cis (**1a**) and trans (**1b**)

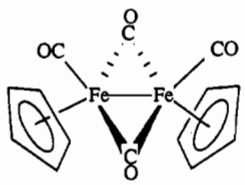

1a

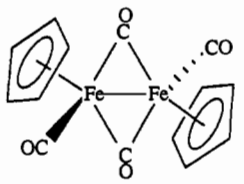

1b

isomers of the dimer, and a single bridging carbonyl peak.[25-27] Similarly, the radical exhibits three peaks, indicating it also exists as a mixture of the cis and trans isomers. The shifts in the terminal carbonyl stretching frequencies to higher energy (by 60 and 68 cm^{-1}) are consistent with the oxidation of the d^7–d^7 binuclear to the one-electron oxidized d^6–d^7 complex, in which the unpaired electron is delocalized over both metals. The relatively large breadth and large shift in the bridging carbonyl stretching frequency (169 cm^{-1}) are unusual and may indicate that the bridging carbonyls may be semibridging in the radical cation.[28] The difference in geometry between the parent and the radical that is evidenced in the large change in the bridging-carbonyl signal may also explain the rather large cyclic voltammetry peak separation of the initial oxidation; a slow change in the structure of the complex upon oxidation would generate a species with a different reduction potential than that which would exist for the radical-cation dimer of the same geometry of the parent.

The observation of only a single bulk oxidation peak, in both methylene chloride and acetonitrile, is consistent with previous kinetic data concerning the interconversion of the two isomers of $[CpFe(CO)_2]_2$. If interconversion of the isomers was slow on the cyclic voltammetry time scale, then two bulk oxidations might be observed, as the two bulk species would likely have slightly different oxidation potentials. However, ^1H NMR experiments show that the isomerization is rapid.[27] Thus, the electrochemistry is best explained by a scheme where one of the isomers, for instance the cis species, is more easily oxidized than the other. As the cis concentration is depleted, it is also rapidly regenerated via the isomerization of the trans complex. Eventually, all of the dimer is consumed by the oxidation of the single isomer. The possible effects of the cis ↔ trans isomerization on the kinetic measurements of the *chemical* oxidation of $[CpFe(CO)_2]_2$ have been considered by Meyer and co-workers.[11]

Our observation of two isomers of $[CpFe(CO)_2]_2^+$ is of additional interest. These species could arise in one of two ways: either the bulk electrolysis potential was sufficient to oxidize both isomers of the parent to radical cations of like geometries or only one isomer of the radical cation is generated at the electrode and this isomer undergoes rapid (on the thin-layer bulk electrolysis time scale) isomerization to generate the cis and trans forms. If the isomerization mechanism for the radical is similar to the proposed mechanism of the parent (i.e., rotation about the iron–iron bond of the unbridged isomer),[27] then the iron–iron half-bond of the unbridged radical cation must be strong enough to hold the complex together during the time it takes for rotation about the bond. At the present time, we have no data to discern these two mechanistic possibilities.

Our direct observation of $[CpFe(CO)_2]_2^+$ in CH_2Cl_2/TBAH lends strong support for an ECE mechanism of the net two-electron oxidation of the parent dimer in acetonitrile but not to a mechanism that is entirely analogous to the ECE mechanism proposed by Kadish for the oxidation of $[CpMo(CO)_3]_2$. The primary difference between the chemistry of these two systems lies in the relative stabilities of the radical-cation dimers. In the molybdenum case, this species decomposes in both coordinating and noncoordinating solvent/electrolyte combinations. In contrast, $[CpFe(CO)_2]_2^+$ is stable in noncoordinating media but decomposes in the presence of nucleophiles. Obviously, the mechanism of the net two-electron oxidation of $[CpFe(CO)_2]_2$ must differ from that of the molybdenum analogue because a nucleophile (better than CH_2Cl_2 or PF_6^-) is required for the oxidation to proceed to completion. The increased stability of $[CpFe(CO)_2]_2^+$ relative to $[CpMo(CO)_3]_2^+$ may be due to the presence of two bridging carbonyl ligands that could help maintain the binuclear structure of the radical. It is likely that the molybdenum analogue has a structure similar to that of the neutral parent complex, with only terminal carbonyl ligands. As a result, the molybdenum–molybdenum bond of order $^1/_2$ in the radical-cation intermediate is probably not strong enough to hold the molybdenum fragments together; the radical then decomposes via heterolytic bond cleavage.

Figure 2 shows that $[CpFe(CO)_2]_2^+$ is irreversibly oxidized at the electrode at 1.28 V. There are two major reduction peaks, at −0.27 and −0.57 V, coupled to this oxidation process. Assignment of these processes was facilitated by additional infrared spectroelectrochemical experiments. Bulk oxidation of the radical cation in the spectroelectrochemical thin cell does not proceed smoothly as passivation of the electrode occurs before the electrolysis is complete. However, the experiment clearly showed that two new sets of peaks grow in as those due to the radical cation decrease in intensity. The new peaks are due to the generation of $[CpFe(CO)_3(PF_6)$ (ν_{CO} = 2126, 2081 cm^{-1}) and $[CpFe(CO)_2(OH_2)](PF_6)$ (ν_{CO} = 2076, 2030 cm^{-1}). The reduction potentials for these cations also match those observed for the reductions coupled to the irreverisble oxidation of $[CpFe(CO)_2]_2^+$ and are assigned to the reduction of these species.[29] The reduction products for both of these cations are the neutral parent dimer and free ligand, i.e., CO and H_2O.

We have given some consideration to the possible routes by which the oxidation of $[CpFe(CO)_2]_2^+$ leads to $[CpFe(CO)_3]^+$ and $[CpFe(CO)_2(OH_2)]^+$. The generation of both of these species is consistent with the initial generation of the 16-electron cation $[CpFe(CO)_2]^+$.[7] While we do not directly observe this species, it is a reasonable intermediate that is similar to the previously isolated $[CpFe(CO)_2](BF_4)$.[30] We believe that this 16-electron iron species rapidly decomposes via two pathways (Scheme I). Because $[CpFe(CO)_2]^+$ is an electron-deficient species, it is expected to behave as a strong Lewis acid; hence, it probably reacts with residual water in the electrolyte to yield the 18-electron $[CpFe(CO)_2(OH_2)](PF_6)$. The other decomposition route of $[CpFe(CO)_2]^+$ generates the tricarbonyl cation. This chemistry parallels that observed for the isoelectronic species $[CpMo(CO)_3]^+$, which decomposes above −10 °C to yield $[CpMo(CO)_4]^+$.[31] Given

(23) Román, E.; Astruc, D. *Inorg. Chem.* **1979**, *18*, 3284.
(24) When solutions of the electrogenerated radical dimer cation were monitored in the IR spectroelectrochemical cell (after completion of the electrolysis), the radical decomposed via disproportionation; we believe that residual water in the electrolyte induces the disproportionation, resulting in the generation of $[CpFe(CO)_2]_2$, and the oxidation products $[CpFe(CO)_3](PF_6)$ and $[CpFe(CO)_2(OH_2)](PF_6)$. See text for further discussion of the ligand-induced disproportionation reactions.
(25) Manning, A. R. *J. Chem. Soc. A* **1968**, 1319.
(26) McArdle, P.; Manning, A. R. *J. Chem. Soc. A* **1970**, 2119.
(27) Bullitt, J. G.; Cotton, F. A.; Marks, T. J. *Inorg. Chem.* **1972**, *11*, 671.
(28) Cotton, F. A.; Wilkinson, G. *Advanced Inorganic Chemistry*, 4th ed.; Wiley-Interscience: New York, 1980; p 1057.
(29) The reduction potentials of $[CpFe(CO)_3](PF_6)$, E_c = −0.54 V, and $[CpFe(CO)_2(OH_2)](PF_6)$, E_c = −0.27 V, were measured from actual samples of these compounds. The latter species was generated electrochemically.[22]
(30) Mattson, B. M.; Graham, W. A. G. *Inorg. Chem.* **1981**, *20*, 3186.

Scheme I. Oxidation of $[CpFe(CO)_2]_2^+$ and Subsequent Reactions

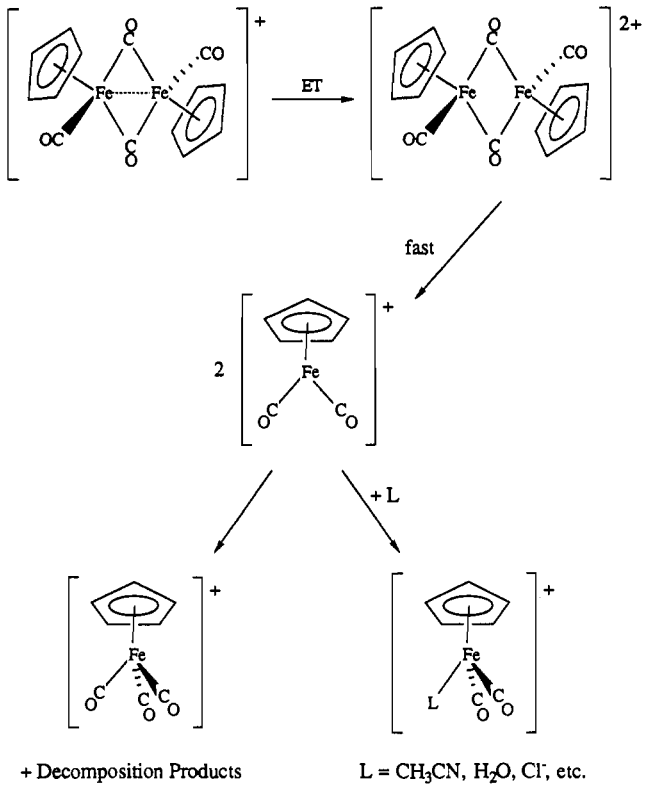

the similarities between the two 16-electron starting species, we believe that the iron compound decomposes in a reaction analogous to one described for the molybdenum system.

It is interesting to note that the tricarbonyl cation has also been generated via the *chemical* oxidation of $[CpFe(CO)_2]_2$ by $NOPF_6$ in methylene chloride, i.e., under noncoordinating conditions.[32] The generation of $[CpFe(CO)_3]^+$ was attributed to an asymmetric oxidative cleavage of the iron–iron bond. While we have no direct evidence to dispute this route to the tricarbonyl, our observations suggest it is not necessary to invoke such a step in the reaction mechanism and that the observed products can be explained by the initial generation and subsequent decomposition of $[CpFe(CO)_2]^+$. Perhaps even more conclusive evidence that the tricarbonyl cation arises from the decomposition of the 16-electron dicarbonyl species comes from an infrared spectroelectrochemical oxidation of $CpFe(CO)_2SnPh_3$ in CH_2Cl_2/TBAH. This species undergoes a net two-electron oxidation in acetonitrile[33] and methylene chloride. In acetonitrile, the iron-containing oxidation product is $[CpFe(CO)_2(NCCH_3)]^+$, which arises from a net two-electron oxidative cleavage of the tin–iron bond. In noncoordinating media, however, the initially formed $[CpFe(CO)_2]^+$ is not stabilized by the coordination of a ligand and decomposes as a result. In the infrared thin cell, the 16-electron dicarbonyl species is not directly observed; instead, one of the major oxidation products is $[CpFe(CO)_3]^+$. Under these conditions, the tricarbonyl can only arise from the reaction of one iron fragment with another iron carbonyl species; an asymmetric oxidative cleavage such as that suggested for the oxidation $[CpFe(CO)_2]_2$ is not possible.

Electrochemistry of $[Cp^*Fe(CO)_2]_2$. The electrochemistry of the permethylated analogue of $[CpFe(CO)_2]_2$ is similar to that of the parent compound in that it exhibits a quasi-reversible one-electron oxidation in CH_2Cl_2/TBAH ($E_{1/2}$ = 0.34 V; i_c/i_a = 0.97; $E_a - E_c$ = 125 mV) and an irreversible net two-electron oxidation in CH_3CN/TBAH (E_a = 0.33 V).[34] The potentials at which these processes occur, and those for analogous processes of related compounds, are summarized in Table I. The oxidation of $[Cp^*Fe(CO)_2]_2$ occurs at a lower potential in both acetonitrile and methylene chloride than does that for the unmethylated analogue. This is attributed to the greater stabilization of the oxidized form of the coupled due to the enhanced electron-donating ability of the Cp* ligand relative to Cp. The irreversible second oxidation process is coupled to two reduction processes in a manner similar to that of the unmethylated dimer, and these reduction peaks are assigned to processes analogous to those described for the $[CpFe(CO)_2]_2$ system. Specifically, a peak at –0.55 V is due to the reduction of $[Cp^*Fe(CO)_2(OH_2)]^+$ and the peak at –0.89 V is due to the reduction of $[Cp^*Fe(CO)_3]^+$.[35]

Table I. Cyclic Voltammetric Peak Potentials (V vs Ag/AgCl) for the Oxidation of Carbonyl-Bridged Iron–Iron Complexes[a]

In CH_2Cl_2/TBAH					
compd	$E°$	$E_a{}^c$	compd	$E°$	$E_a{}^c$
$[CpFe(CO)_2]_2$	0.68	1.28	$[Cp^*Fe(CO)_2]_2$	0.34	1.16

In CH_3CN/TBAH			
compd	$E_{p,a}{}^d$	compd	$E_{p,a}{}^d$
$[CpFe(CO)_2]_2{}^d$	0.55	$[Cp^*Fe(CO)_2]_2$	0.33

[a] Scan rate = 100 mV/s unless otherwise noted. [b] This designation refers to the direct oxidation of the radical-cation dimer species. [c] The anodic peak corresponds to the irreversible net two-electron oxidation of these compounds. [d] Scan rate = 250 mV/s.

Data for the electrooxidation of $[Cp^*Fe(CO)_2]_2$ were also obtained in the infrared spectroelectrochemical thin cell.[34] As was the case with the unmethylated complex, an isosbestic conversion of the parent (ν_{CO} 1747, 1922 cm^{-1}) to the radical cation (ν_{CO} 1884, 1987 cm^{-1}) is observed. In this case, the parent complex has only a single peak in the terminal carbonyl region because only the trans isomer is present in solution;[37] similarly, the single terminal carbonyl peak for the radical cation indicates that a single isomer is present for the oxidation product as well.

We have further characterized the radical species $[CpFe(CO)_2]_2^+$ and $[Cp^*Fe(CO)_2]_2^+$ by EPR spectroscopy. X-Band EPR spectra[34] for these species in frozen CH_2Cl_2/TBAH solutions obtained at –170 °C show two signals, corresponding to radicals that are randomly oriented with respect to the applied magnetic field. These nearly axial EPR spectra are similar to ones obtained for other binuclear radical species with partially occupied σ or σ^* orbitals.[38] The measured g values ($[CpFe(CO)_2]_2^+$, $g_\parallel$ = 2.004, $g_\perp$ = 2.084; $[Cp^*Fe(CO)_2]_2$, $g_\parallel$ = 1.999, $g_\perp$ = 2.088) are consistent with radical species in which the unpaired electron is shared by the metals via a σ-bonding interaction. For both species, the $g_\parallel$ signal is thought to be due to the principal iron–iron axis. No hyperfine coupling is observed in these spectra. The minor features of the otherwise broad signals at higher g values have not been assigned. The measured g values are similar to those obtained by Haines and du Preez for the μ-dppe- and μ-dppm-substituted analogues.[10]

Mechanism of the Ligand-Induced Disproportionations. As mentioned earlier, the binuclear radical dimers $[CpFe(CO)_2]_2^+$ and $[Cp^*Fe(CO)_2]_2^+$ are analogous to a previously characterized radical cation, $\{[CpFe(CO)]_2(\mu\text{-dppe})\}(PF_6)$, which can be generated via chemical[10] or electrochemical oxidation of the neutral parent complex.[8,9] The cyclic voltammogram of $[CpFe(CO)]_2(\mu\text{-dppe})$ in CH_3CN/TBAH exhibits a quasi-reversible oxidation peak, in contrast to the irreversible oxidation peaks of the un-

(31) Beck, W.; Scholter, K. *Z. Naturforsch., B: Anorg. Chem., Org. Chem.* **1978**, *33B*, 1214.
(32) Reimann, R. H.; Singleton, E. *J. Organomet. Chem.* **1971**, *32*, C44.
(33) Bullock, J. P.; Pallazotto, M. C.; Mann, K. R. *Inorg. Chem.* **1990**, *29*, 4413.
(34) See supplementary material.
(35) The identity of these species was confirmed by IR spectroelectrochemical oxidation of the radical dimer cation. ($[Cp^*Fe(CO)_3](PF_6)$[36], ν_{CO} 2102, 2050 cm^{-1}; $[Cp^*Fe(CO)_2(OH_2)](PF_6)$, ν_{CO} = 2147, 1997 cm^{-1}).
(36) Catheline, D.; Astruc, D. *J. Organomet. Chem.* **1982**, *226*, C52.
(37) Teller, R. G.; Williams, J. M. *Inorg. Chem.* **1980**, *19*, 2773.
(38) For example, several binuclear rhodium radicals show similar spectra. See: (a) Le, J. C.; Chavan, L. K. C.; Bear, J. L.; Kadish, K. M. *J. Am. Chem. Soc.* **1985**, *107*, 7195. (b) Boyd, D. C.; Matsch, P. A.; Mixa, M. M.; Mann, K. R. *Inorg. Chem.* **1986**, *25*, 3331. (c) Piraino, P.; Bruno, G.; Tresoldi, G.; Schiavo, S. L.; Zanello, P. *Inorg. Chem.* **1987**, *26*, 91.

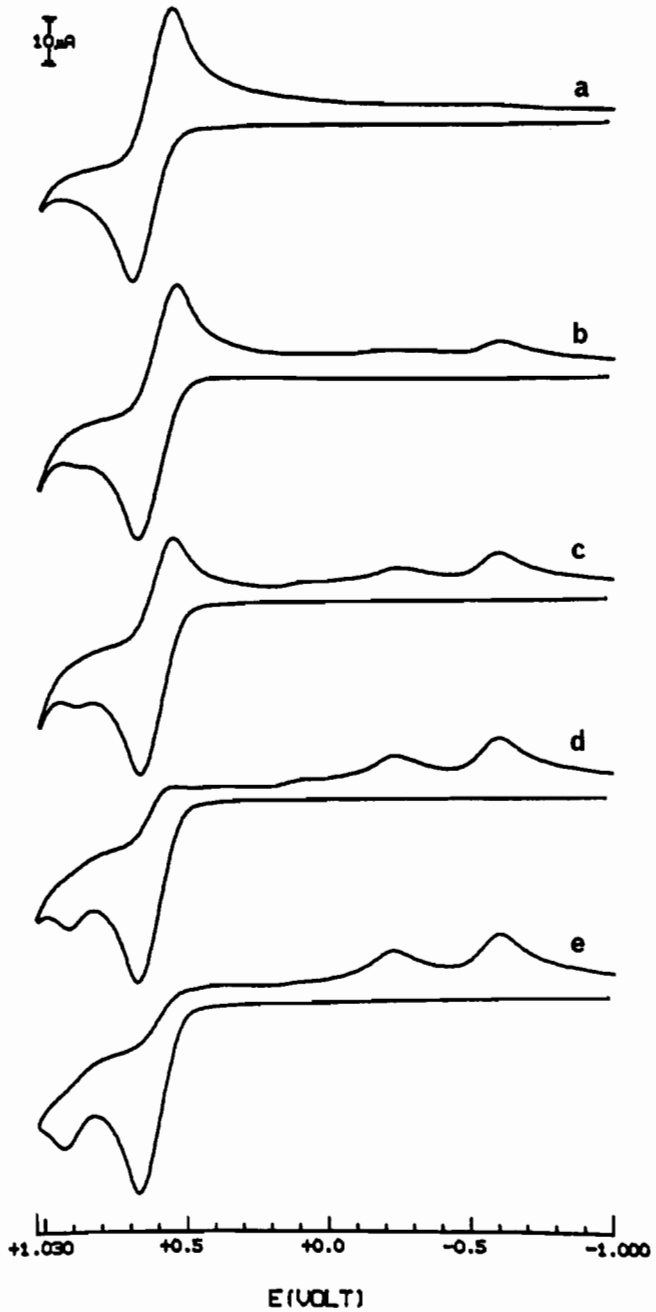

Figure 4. Cyclic voltammograms of a 1.06 mM solution of $[CpFe(CO)_2]_2$ in CH_2Cl_2/TBAH as increments of acetonitrile are added. The number of added equivalents of acetonitrile in each case is as follows: (a) 0.0; (b) 0.1; (c) 0.2; (d) 0.4; (e) 0.8. The scan rate is 200 mV/s in each experiment.

substituted complexes described above. The enhanced electrochemical reversibility of the dppe-substituted species is a manifestation of the much slower reaction of the electrogenerated radical cation with acetonitrile. Both $[CpFe(CO)_2]_2^+$ and $[Cp^*Fe(CO)_2]_2^+$ undergo rapid ligand-induced disproportionations (eq 5). The extreme sensitivity of these species toward potential

$$2[CpFe(CO)_2]_2^+ + 2L \rightarrow [CpFe(CO)_2]_2 + 2[CpFe(CO)_2L]^+ \quad (5)$$

$$L = CH_3CN,\ H_2O,\ Cl^-,\ \text{etc.}$$

ligands helps explain their hitherto elusive character. For example, the reversibility of the $[CpFe(CO)_2]_2$ oxidation peak is markedly diminished in the presence of even *subequivalent* concentrations of acetonitrile (Figure 4).

We have explored the mechanism of these ligand-induced net disporportionation reactions by both electrochemical and spectroscopic techniques. On the basis of these experiments and

Scheme II. Proposed Ligand-Induced Disproportionation Mechanism of $[CpFe(CO)_2]_2$ and $[Cp^*Fe(CO)_2]_2$

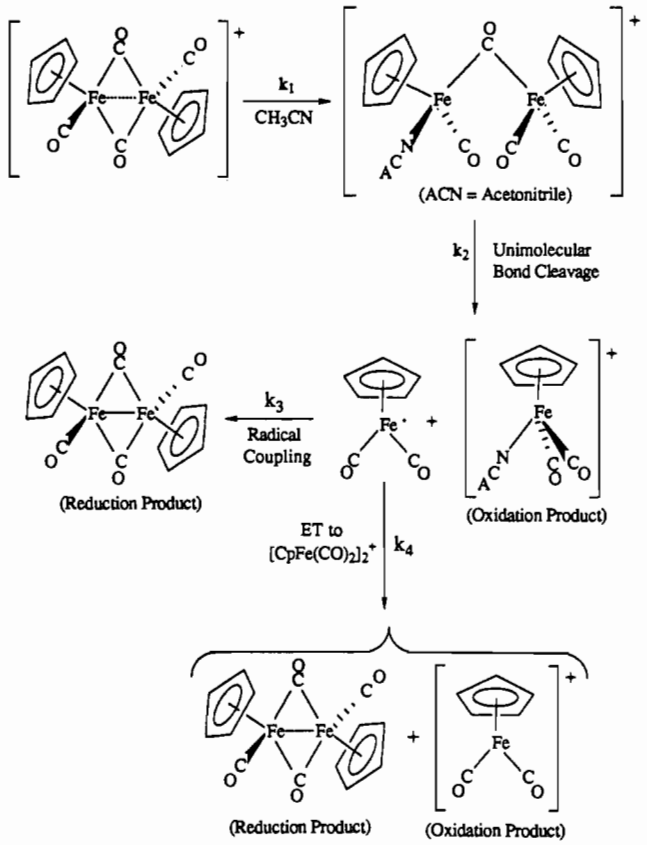

qualitative observations concerning the reactivity of the radical cations, we propose a mechanism of this reaction in Scheme II. Briefly, the radical cation binds an acetonitrile ligand to generate a carbonyl-bridged binuclear species. This intermediate complex then decomposes in a first-order process to yield one 17-electron monomer radical and one of the final oxidation products, $[CpFe(CO)_2(NCCH_3)]^+$. The neutral radical then reacts to regenerate the neutral parent complex by one of two routes: coupling with another radical fragment in a second-order process or electron-transfer reaction with a radical dimer cation to reduce the dimer and make the 16-electron species $[CpFe(CO)_2]^+$. Thus, we believe that the reactivity of this radical fragment is dependent on the nature of the major species in solution; if the major species is the binuclear radical cation, the electron-transfer reaction predominates, but if the unreactive dimer is the major species, radical coupling is favored. Finally, the 16-electron cation undergoes its own sequence of condition-dependent decomposition reactions to make either a $[CpFe(CO)_3]^+$ or $[CpFe(CO)_2L]^+$ complex. If the disproportionation takes place in a large excess of acetonitrile, then the oxidation product of the reaction is exclusively $[CpFe(CO)_2(NCCH_3)]^+$; however, if low concentrations of acetonitrile are employed to induce the disproportionation, i.e., the concentration of acetonitrile is largely exhausted by the first step of the reaction, then the generated $[CpFe(CO)_2]^+$ decomposes, as outlined in Scheme I, to yield $[CpFe(CO)_2(OH_2)]^+$ and $[CpFe(CO)_3]^+$. This explains why two reduction waves, one for $[CpFe(CO)_2(NCCH_3)]^+$ and one for $[CpFe(CO)_2(OH_2)]^+$, are coupled to the oxidation of $[CpFe(CO)_2]_2$ in the presence of subequivalent amounts of acetonitrile (Figure 4). At higher acetonitrile concentrations, the peak due to the reduction of the aquo complex gets smaller relative to the acetonitrile-adduct peak and eventually is not observed.

The observed electrochemistry of $[CpFe(CO)_2]_2$ under a variety of conditions is consistent with the chemistry outlined in Scheme II. In both coordinating and noncoordinating media, $[CpFe(CO)_2]_2$ is initially oxidized by one electron to give the binuclear radical cation. In coordinating solvent/electrolytes, this species

Scheme III. Chemistry of $\{[CpFe(CO)_2](CH_3CN)\}^+$

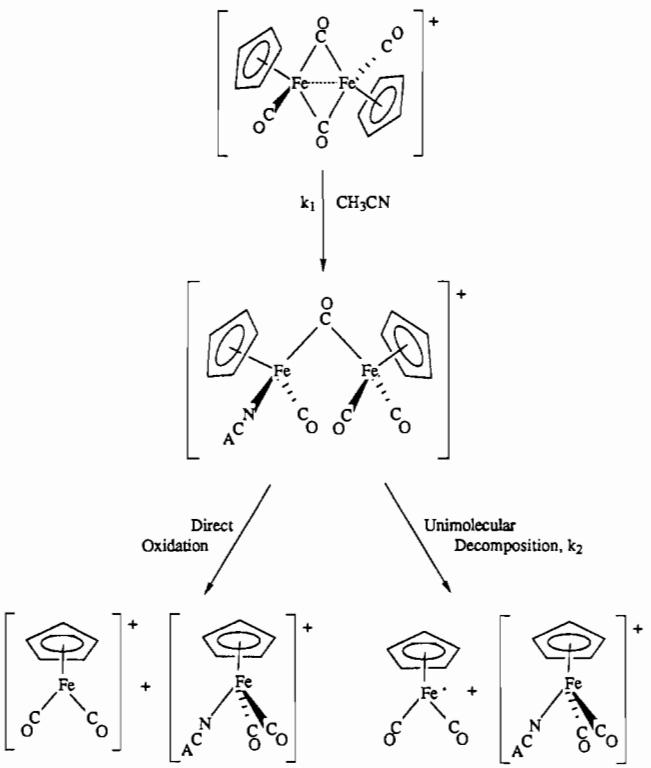

reacts with a nucleophile, either a solvent molecule or a supporting anion (e.g., acetonitrile, acetone, chloride, perchlorate, etc.), to ultimately regenerate a half equiv of the starting dimer. The regenerated dimer is then oxidized at the electrode and the cycle begins again until all of the starting dimer is consumed and the net result is an irreversible net two-electron oxidation of $[CpFe(CO)_2]_2$.[39] However, if the oxidation of $[CpFe(CO)_2]_2$ takes place in the absence of a suitable ligand, the radical-cation dimer is long-lived and can be directly oxidized at the electrode in a second one-electron process.

Additional evidence in support for this mechanism can be summarized as follows: (1) $[CpFe(CO)_2]_2^+$ reacts with acetonitrile to yield an intermediate species that is observable by cyclic voltammetry; (2) $[Cp^*Fe(CO)_2]_2^+$ reacts with acetonitrile in a reaction that is first order in both radical dimer and acetonitrile; (3) qualitative observations strongly suggest that $Cp^*Fe(CO)_2^\bullet$ radicals are generated upon the reaction of $[Cp^*Fe(CO)_2]_2^+$ with acetonitrile.

These points are explained in greater detail below. Cyclic voltammetry clearly shows that electrogenerated $[CpFe(CO)_2]_2^+$ reacts with acetonitrile to generate a new species. Figure 4 shows the cyclic voltammograms of a solution of $[CpFe(CO)_2]_2$ at various stages of an acetonitrile titration; before any acetonitrile is added, the solution exhibits only the quasi-reversible oxidation peak of the neutral dimer. When small amounts of acetonitrile are added to the solution, a new anodic peak emerges at 0.92 V, at a potential positive of the bulk oxidation. A scan rate study of this peak showed that the relative size of the intermediate oxidation peak decreases with slower scan rates. Finally, the size of this peak initially increases with increasing acetonitrile concentrations (at the expense of the second one-electron peak of the bulk species), but at significantly higher concentrations of acetonitrile ($>\sim 2$ equiv/dimer) the peak current maximizes and starts to fall. At high concentrations of acetonitrile this process is not observable; for example, in CH_3CN/TBAH no trace of this peak is seen (see Figure 1).

(39) Another explanation of the current enhancement of the oxidation peak that is seen in coordinating media is that the species being oxidized at the electrode is not the regenerated dimer at all, but instead the 17-electron radical $CpFe(CO)_2^\bullet$.

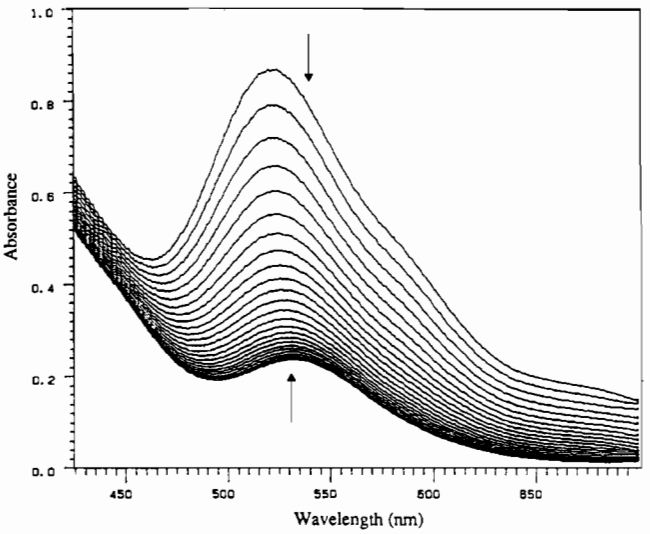

Figure 5. Visible spectral changes observed during the reaction of an approximately 0.20 mM solution of $[Cp^*Fe(CO)_2]_2^+$ in CH_2Cl_2/TBAH with a 50 mM solution of acetonitrile, also in CH_2Cl_2/TBAH. The radical peak at 518 nm is rapidly diminished as the neutral dimer $[Cp^*Fe(CO)_2]_2$ (λ_{max} = 535 nm) is generated in the disproportionation. The solution turns from deep purple to orange-red in this reaction. The spectra in the series were taken at 0.024-s intervals.

The above observations are consistent with the chemistry outlined in Scheme III. The extreme sensitivity of the reversibility of the bulk oxidation to acetonitrile indicates that the nucleophilic attack of the electrogenerated $[CpFe(CO)_2]_2^+$ is rapid and nearly quantitative. The appearance of a new peak clearly indicates that a species is generated in solution other than $[CpFe(CO)_2]_2^+$ or the final oxidation product $[CpFe(CO)_2(NCCH_3)](PF_6)$. We assign the new peak to the oxidation of the intermediate species $\{[CpFe(CO)_2]_2(NCCH_3)\}(PF_6)$ (this complex may or may not have a direct iron–iron interaction; a discussion of the possible structure of the intermediate is presented below). Moreover, the decrease in the peak current at slower scan rates indicates that the intermediate undergoes a relatively slow decomposition reaction on the cyclic voltammetry time scale. At slower scan rates the reaction becomes fast enough, relative to the sweep time, to deplete the concentration of the intermediate near the electrode. In terms of the two pathways for intermediate decomposition drawn in Scheme III, at fast scan rates, the intermediate is directly oxidized at the electrode, while at slower scan rates the unimolecular decomposition route predominates. The eventual disappearance of the intermediate oxidation peak at higher acetonitrile concentrations is due to an enhancement of the intermediate decomposition rate, perhaps by the association of additional acetonitrile molecules.

The second point made above concerns the order of the ligand-induced disproportionation reaction in $[Cp^*Fe(CO)_2]_2^+$ and acetonitrile. These reaction orders were determined by a series of stopped-flow experiments in the visible spectral region.[40] All stopped-flow experiments were performed under pseudo-first-order conditions in acetonitrile. In these experiments, deep purple solutions of the binuclear radical cation quickly changed to or-

(40) Stopped-flow experiments in the visible spectral region were limited to the study of $[Cp^*Fe(CO)_2]_2$ because of the difficulty in cleanly handling bulk solutions of the unmethylated binuclear radical cation. Solutions of $[Cp^*Fe(CO)_2]_2^+$ were generated via exhaustive electrolysis of the neutral parent at a potential between the two oxidation processes; these electrolyses proceeded relatively smoothly, with only minor decomposition of the radical (the primary decomposition product was $[Cp^*Fe(CO)_3](PF_6)$). Large-scale bulk oxidations of $[CpFe(CO)_2]_2$ did not cleanly generate the radical dimer. Although most of the dimer was converted to the radical dimer, decomposition occurred to a greater extent than with the Cp* compound, as evidenced by a small amount of a black precipitate that developed over the course of the electrolysis. A significant amount of $[CpFe(CO)_3](PF_6)$ was also generated. The resulting solutions proved to be extremely sensitive to handling and could not be studied by stopped-flow experiments.

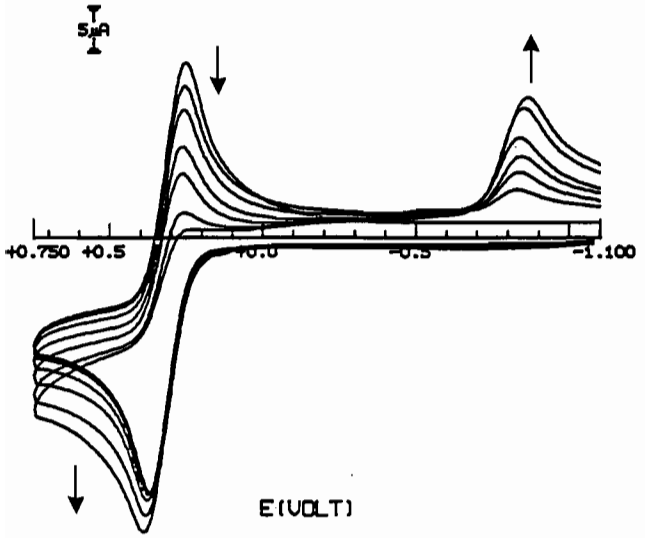

Figure 6. Cyclic voltammograms of a 0.98 mM solution of $[Cp^*Fe(CO)_2]_2$ at different stages of an acetonitrile titration. The arrows indicate the direction of change in the peak heights. The coupled reduction peak at −0.84 V is due to $[Cp^*Fe(CO)_2(NCCH_3)]^+$. The ratio of acetonitrile to iron dimer in the series is as follows: 0.0, 1.2, 2.5, 4.9, 7.7, 12.1, 19.1, and 38.3.

ange-red upon addition of acetonitrile. The changes in the visible spectrum of a solution of $[Cp^*Fe(CO)_2]_2(PF_6)$ as it reacts with an excess of acetonitrile (approximately 250 equiv per binuclear radical) are shown in Figure 5. The spectra were taken at 0.024-s intervals. The radical cation peak at 518 nm, and shoulders at 582 and 682 nm, decrease in intensity as those due to the products emerge. The peak that grows in at 535 nm is due to the neutral parent complex $[Cp^*Fe(CO)_2]_2$. The first-order plot[34] of the change in absorbance measured at the radical peak maximum (integrated over a 10-nm window, from 515–525 nm) is linear ($r^2 = 0.9991$) over the first 10 half-lives.[41] The reaction is first order in $[Cp^*Fe(CO)_2]_2^+$. The slope of the first-order plots varies with acetonitrile concentration. A plot of k_{obs} against the concentration of acetonitrile used yields a straight line.[34] Thus, the reaction is also first order in acetonitrile. From the slope of the least-squares line, a second-order rate constant of 118 (± 2) M^{-1} s^{-1} is obtained. This rate constant corresponds to k_1 in Schemes II and III.

No intermediate species is observed in the stopped-flow experiments as the absorbance of the neutral parent dimer grows in first order in this reaction. This implies that all of the reactions following the rate-determining step shown in Scheme III must be very fast on this time scale (i.e., k_2, k_3, and k_4 are very large). Consequently, the proposed carbonyl-bridged intermediate in the Cp* system must be extremely short-lived under the stopped-flow conditions, in contrast to $\{[CpFe(CO)_2]_2(NCCH_3)\}^+$. However, the cyclic voltammograms of a solution of $[Cp^*Fe(CO)_2]_2$ with small amounts of added acetonitrile (Figure 6) *are* consistent with the generation of a short-lived intermediate complex. As the reversibility of the iron dimer oxidation is diminished with increasing acetonitrile concentration, no additional anodic or cathodic peak attributable to the oxidation or reduction of an intermediate is observed; the coupled cathodic peak that grows in during the titration is due to the reduction of $[Cp^*Fe(CO)_2(NCCH_3)](PF_6)$. As seen in Figure 6, even though no distinct intermediate peak is observed, the peak current and the current at the diffusion plateau of the cyclic voltammograms are higher in solutions with greater concentrations of acetonitrile. We attribute our observation to the relatively slow (on the cyclic voltammetry time scale) formation of a complex that is rapidly oxidized at the bulk peak potential. The rate of the reaction of $[Cp^*Fe(CO)_2]_2^+$ with acetonitrile, to form the more easily oxidized species, limits the additional current passed at the electrode; higher concentrations of acetonitrile result in faster reaction rates of the radical dimer, with concomitant increases in the peak and diffusion plateau currents. The identity of the complex that causes the additional current in the diffusion plateau is unknown; it could be the carbonyl-bridged intermediate, the 17-electron radical species, or regenerated parent dimer.

The third and final point made above indicates that the decomposition products of $[Cp^*Fe(CO)_2]_2^+$ are best explained if the 17-electron radical species $Cp^*Fe(CO)_2^\bullet$ is generated as an intermediate. Specifically, when $[Cp^*Fe(CO)_2]_2$ is bulk electrolyzed in the presence of excess acetonitrile in a solution of CH_2Cl_2/TBAH (under continuous stirring), the concentration of $[Cp^*Fe(CO)_2]_2$ was exhausted when only about 1.5 electrons/dimer were removed. This compares to 2 electrons/dimer expected for the oxidation of the neutral dimer to $[Cp^*Fe(CO)_2(NCCH_3)](PF_6)$. The infrared spectrum of the solution after completion of the electrolysis revealed that, in addition to the expected oxidation product, a significant amount of the dimer was oxidized to $Cp^*Fe(CO)_2Cl$. The source of the chloro adduct cannot be a direct reaction of the electrogenerated radical cation dimer with the chlorinated solvent, because solutions of $[Cp^*Fe(CO)_2]_2^+$ can be cleanly generated via bulk electrolysis of the neutral dimer in CH_2Cl_2/TBAH and are stable for extended periods, with no production of $Cp^*Fe(CO)_2Cl$. However, it is well established that $CpFe(CO)_2^\bullet$, generated via photolysis of the parent dimer, reacts with chlorinated solvents (e.g., CCl_4, $CHCl_3$, CH_2Cl_2, etc.) to yield $CpFe(CO)_2Cl$.[42,43] The better reductant, $Cp^*Fe(CO)_2^\bullet$, is expected to abstract $Cl^\bullet$ from solvents even more readily because such halide abstractions are thought to proceed via mechanisms that have significant electron-transfer components.[44] The result of the bulk electrolysis strongly suggests that $Cp^*Fe(CO)_2^\bullet$ is generated from the reaction of the electrogenerated $[Cp^*Fe(CO)_2]_2^+$ with acetonitrile. Because all of the iron exists in the +2 oxidation state after the reaction, and not enough charge was passed at the electrode to account for this conversion, the difficiency of charge is attributed to oxidation of $Cp^*Fe(CO)_2^\bullet$ by methylene chloride.

Another observation consistent with the generation of $Cp^*Fe(CO)_2^\bullet$ during the ligand-induced disproportionation is that the neutral parent dimer is regenerated *only* if the reaction between $[Cp^*Fe(CO)_2]_2^+$ and acetonitrile is performed under anaerobic conditions. While neither the reactant, $[Cp^*Fe(CO)_2]_2^+$, nor the product of interest, $[Cp^*Fe(CO)_2]_2$, is particularly air-sensitive over short periods of time, the reaction does not yield the expected product if the solutions contain oxygen. Therefore, the reaction must proceed via an air-sensitive intermediate. It has been established that species such as $Cp^*Fe(CO)_2^\bullet$ are good reducing agents;[45] hence, their generation in a reaction pathway would be manifested in the products of that reaction being dependent on the presence of oxidizing agents.[46]

The above discussion describes our evidence in support of the mechanism outlined in Scheme II. While we hold that the ligand-induced disproportionations of $[CpFe(CO)_2]_2^+$ and $[Cp^*Fe(CO)_2]_2^+$ follow analogous mechanisms, there are still

(41) Extraction of rate information from these data was complicated by the observation of a concurrent second-order process. The rate information was obtained by fitting the data to the curve generated by simultaneous first- and second-order decays of independent species; the modelling was done via a nonlinear least-squares fitting program, with the first- and second-order rate constants, as well as the initial absorbances of the two reacting species and the final absorbance of the solution, being treated as variables. The initial absorbance due to the second-order process was generally less than 5% of the total initial absorbance. The second-order process is believed to be a reaction involving residual oxygen in the solutions.

(42) Gianotti, C.; Merle, G. *J. Organomet. Chem.* **1976**, *105*, 97.
(43) Abrahamson, H. B.; Palazotto, M. C.; Reichel, C. L.; Wrighton, M. S. *J. Am. Chem. Soc.* **1979**, *101*, 4123.
(44) Lee, K.-W.; Brown, T. L. *J. Am. Chem. Soc.* **1987**, *109*, 3269.
(45) Hepp, A. F.; Wrighton, M. S. *J. Am. Chem. Soc.* **1981**, *103*, 1258.
(46) Another possible interpretation of this observation is that the proposed intermediate species $\{[Cp^*Fe(CO)_2]_2(NCCH_3)\}^+$ is the air-sensitive species in this mechanism. We do not consider this likely on the basis of oxidation potential of the unmethylated analogue of this species, which is positive of that of the neutral parent dimer.

significant differences between the chemistry of the two species. Specifically, while the intermediate complex $\{[CpFe(CO)_2]_2(NCCH_3)\}^+$ is observed via cyclic voltammetry, we have no direct evidence that the permethylated analogue is generated. This does not necessarily mean the reactions occur via different mechanisms. Instead, this observation can be explained by the relative differences in the rates k_1 and k_2 in Scheme II. For $[CpFe(CO)_2]_2$, the direct observation of the intermediate indicates that its formation is faster than its subsequent decomposition; i.e., $k_1[[CpFe(CO)_2]_2^+][CH_3CN]) > k_2[\{[CpFe(CO)_2]_2(NCCH_3)\}^+]$. For $[Cp^*Fe(CO)_2]_2$, the intermediate is not observed either spectroscopically or electrochemically; thus, $k_1[[Cp^*Fe(CO)_2]_2^+][CH_3CN]) \ll k_2[\{[CpFe(CO)_2]_2(NCCH_3)\}^+]$. We have only measured one of the above rate constants (i.e., k_1 of the disproportionation involving $[Cp^*Fe(CO)_2]_2^+$). However, we have made a rough estimate of the value of k_1 for the unmethylated analogue via double potential-step chronocoulometry. A plot of Q_r/Q_f (the charge passed in the reverse and forward steps of the experiment, respectively), which is a measure of the reversibility of a bulk process, against log ($[[CpFe(CO)_2]_2][\tau]$) (τ = step time) yields a curve,[34] whose shape reveals mechanistic information.[47] Unfortunately, the generation of a theoretical curve based on our complicated proposed mechanism was beyond the scope of this work. We observe that the time scale of the reaction between $[CpFe(CO)_2]_2^+$ and acetonitrile is consistent with a second-order rate constant of 10^4 M^{-1} s^{-1}. This estimate is based on the position of the inflection point of the curve along the x axis.[48] This rate constant compares to 120 M^{-1} s^{-1} for the reaction between $[Cp^*Fe(CO)_2]_2^+$ and acetonitrile; thus, the reaction of the unmethylated radical dimer is roughly 2 orders of magnitude greater than that of $[Cp^*Fe(CO)_2]_2^+$. This may explain, in part, why the intermediate complex is observed in the oxidation of $[CpFe(CO)_2]_2$ but not in that of $[Cp^*Fe(CO)_2]_2$.

While the cyclic voltammetry data clearly show that an intermediate species is generated upon the oxidation of $[CpFe(CO)_2]_2$ in the presence of acetonitrile, the exact structure of the intermediate is not known. An attempt to characterize this species via infrared spectroelectrochemistry was unsuccessful, perhaps because the oxidation potential of the intermediate is too close to that of the bulk process or, alternatively, the intermediate decomposes at a rate that is much faster relative to the thin-cell bulk electrolysis time scale than it is to the cyclic voltammetry time scale. Our assignment of the intermediate species as $\{[CpFe(CO)_2]_2(NCCH_3)\}^+$ (**2**) is based on a similar, although not

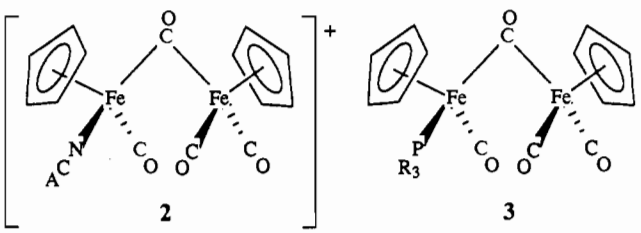

entirely analogous, species observed by other workers. The complex $[Cp_2Fe_2(CO)_3(PR_3)](\mu\text{-}CO)$ (**3**) has been proposed as an intermediate in the generation of $[Cp_2Fe_2(CO)_3(PR_3)]$ via the photolysis of $[CpFe(CO)_2]_2$ in the presence of phosphines.[49] Unlike **3**, which is a 36-electron species with no formal iron–iron

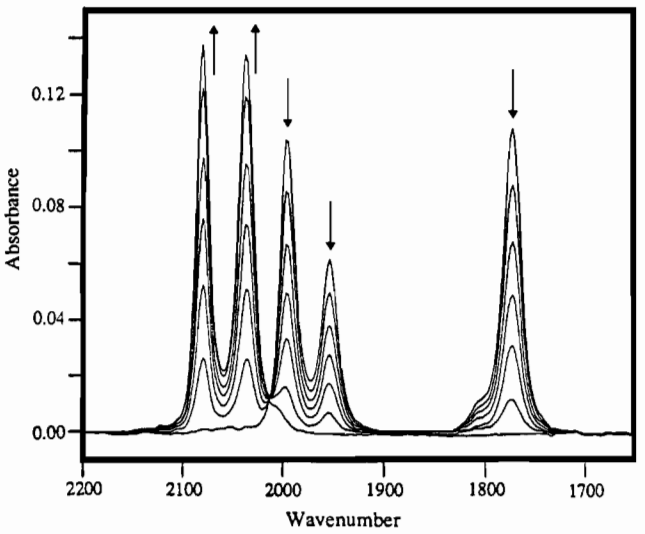

Figure 7. Infrared spectral changes observed upon oxidation of a solution of $[CpFe(CO)_2]_2$ in CH_2Cl_2/TBAH in the presence of approximately 40 equiv of acetonitrile. The electrolysis product is $[CpFe(CO)_2(NCCH_3)]^+$. The arrows indicate the direction of change.

bond, **2** is an electron-deficient (35-electron) binuclear radical cation. As such, there may be a formal iron–iron bond of order $^1/_2$ that could stabilize the complex, but we have no electronic spectra to help ascertain the nature of the metal–metal interaction in this complex.

It is interesting to consider the pathway by which $\{[CpFe(CO)_2]_2(NCCH_3)\}^+$ decomposes (Scheme III). Assuming that the oxidation of $[CpFe(CO)_2]_2$ in the presence of acetonitrile proceeds via this intermediate, the observed products reveal mechanistic information concerning the cleavage of $\{[CpFe(CO)_2]_2(NCCH_3)\}^+$. Figure 7 shows the infrared spectral changes accompanying the oxidation of $[CpFe(CO)_2]_2$ in CH_2Cl_2/TBAH in the presence of approximately 40 equiv of acetonitrile. The bulk oxidation cleanly generates $[CpFe(CO)_2(NCCH_3)]^+$, the oxidation product of a net *symmetric* two-electron oxidative bond cleavage. The oxidation products that would result from a net *asymmetric* bond cleavage are $[CpFe(CO)_3]^+$ and $[CpFe(CO)(NCCH_3)_2]^+$. In order to generate the observed products, the bridging carbonyl bond of $Cp(CO)_2Fe\text{–}(\mu\text{-}CO)^+$, as opposed to the adjacent iron bond, must always be the one broken (i.e., eq 6 must occur to the exclusion of eq 7). If the adjacent

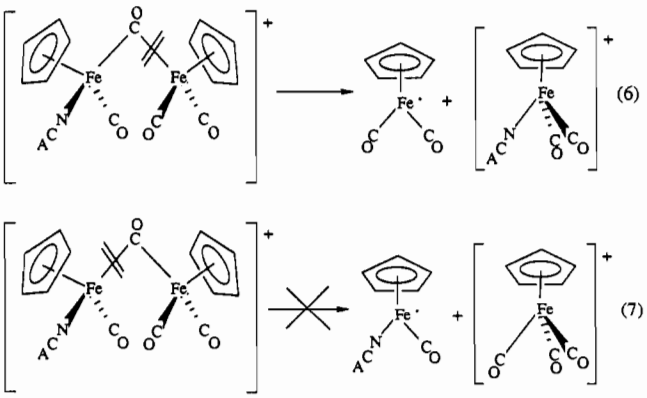

iron–carbonyl bond were to break, $[CpFe(CO)_3]^+$ would be one of the final oxidation products. This is can be understood on the basis of the relative stabilities of the products generated by the two possible pathways if positive charge is centered on the species with the better electron-donating ligand.

Before ending the discussion of the ligand-induced disproportionation mechanism, it is interesting to consider the mechanisms proposed by Meyer and co-workers for the chemical oxidation of $[CpFe(CO)_2]_2$ in acetonitrile.[11] In their work, three mechanisms for the net two-electron oxidation of the dimer were proposed,

(47) Hanafey, M. K.; Scott, R. L.; Ridgway, T. H.; Reilley, C. N. *Anal. Chem.* **1978**, *50*, 116.

(48) The step experiments were performed by adding a stock solution of $[CpFe(CO)_2]_2$ and CH_3CN to the bulk solution; a ratio of acetonitrile to iron dimer of 0.18 was maintained throughout the experiment. The ratio of the effective concentrations, $(C_{acetonitrile})(D_{acetonitrile})^{1/2}/(C_{dimer})(D_{dimer})^{1/2}$, where D is the diffusion coefficient of each species (as estimated by the molecular volumes via the Stokes–Einstein equation), was 0.40 acetonitrile/dimer. A plot of Q_r/Q_f vs log $[[CpFe(CO)_2]_2][\tau]$ (concentration in moles/liter; τ is the step time, in seconds) was generated and the inflection point estimated. The theoretical inflection point for the working curve of the operative mechanism is assumed to occur where log $[k][[CpFe(CO)_2]_2][\tau]$ equals zero.

(49) Tyler, D. R.; Schmidt, M. A.; Gray, H. B. *J. Am. Chem. Soc.* **1983**, *105*, 6018.

Table II. Infrared Stretching Frequencies of $[CpFe(CO)_2]_2$, Related Complexes, and Their Radical-Cation Analogues[a]

compd	parent ν_{CO}	radical cation ν_{CO}
$[CpFe(CO)_2]_2$		
terminal	1955, 1995	2023, 2055
bridging	1773	1934
$[Cp^*Fe(CO)_2]_2$		
terminal	1922	1987
bridging	1747	1884

[a] Measured in CH_2Cl_2/TBAH; values in cm^{-1}.

all of which proceed through the binuclear radical cation, although no behavior attributable to the generation of this intermediate was observed in their kinetic studies. The mechanisms were (a) direct oxidation of the binuclear radical, (b) initial dissociation followed by oxidation of the resulting 17-electron radical, and (c) a second-order disproportionation of the binuclear radicals. Of these three mechanisms, the current work unambiguously rules out the third. It is, however, more difficult to distinguish between the first two pathways, particularly since their kinetic studies were done in acetonitrile whereas all of our work was carried out in methylene chloride. Nevertheless, we believe that mechanism b best describes the chemical oxidation of $[CpFe(CO)_2]_2$, because, as stated earlier, the peak due to the oxidation of the intermediate complex, $\{[CpFe(CO)_2]_2(NCCH_3)\}^+$, decreases in size, after reaching a maximum value, with higher acetonitrile concentrations. The intermediate is not stable in the presence of excess acetonitrile and, in accord with mechanism b, rapidly dissociates. Mechanism a could be the operative mechanism provided the direct oxidation of the intermediate complex is much faster than the initial oxidation to the binuclear radical cation, which was measured to be $\sim 10^4$ M^{-1} s^{-1}.[11]

Conclusions

The electrochemistry of $[CpFe(CO)_2]_2$ and the related species $[Cp^*Fe(CO)_2]_2$ was reexamined under a variety of conditions. Both compounds exhibit irreversible net two-electron oxidations in CH_3CN/TBAH with $E_{p,a}$ = 0.68 and 0.33 V vs AgCl/Ag, respectively. The complexes are symmetrically cleaved via this process to yield the corresponding 18-electron acetonitrile-adduct cations. These binuclear species also undergo quasi-reversible one-electron oxidations in CH_2Cl_2/TBAH to generate the corresponding binuclear radical cations at 0.68 and 0.34 V, respectively. The radical-cation species were generated and characterized via infrared spectroelectrochemistry. $[CpFe(CO)_2]_2^+$ exists as a mixture of the cis and trans carbonyl-bridged isomers in solution with ν(CO) at 2023, 2055, and 1934 cm^{-1}, while $[Cp^*Fe(CO)_2]_2^+$ with ν(CO) at 1987 and 1884 cm^{-1} exists exclusively as the trans isomer in solution (Table II). The unsubstituted radical cations were further characterized by EPR spectroscopy. $[CpFe(CO)_2]_2^+$ has $g_\parallel$ = 2.004 and $g_\perp$ = 2.084, while $[Cp^*Fe(CO)_2]_2^+$ has $g_\parallel$ = 1.999 and $g_\perp$ = 2.088. $[CpFe(CO)_2]_2^+$ has long been invoked as the initial oxidation product of the parent dimer but had never been cleanly generated or characterized prior to this work. The binuclear radical cations are susceptible to rapid ligand-induced disproportionation reactions that were studied via spectroscopic and electrochemical methods. The results of these studies suggest that the mechanisms of these reactions involve the generation and subsequent decomposition of acetonitrile adducts of the binuclear radical-cation species of the form $\{[CpFe(CO)_2]_2(NCCH_3)\}^+$. For the Cp* compound, the intermediate is short-lived. Stopped-flow measurements of the reaction of $[Cp^*Fe(CO)_2]_2^+$ with CH_3CN showed that the reaction is first order in $[[Cp^*Fe(CO)_2]_2^+$ and $[CH_3CN]$ with k = 118 (±2) M^{-1} s^{-1}. Cyclic voltammetry studies detected the parent intermediate $[CpFe(CO)_2]_2(NCCH_3)]^+$. The initially formed decomposition products of the acetonitrile adduct of the binuclear radical in each case (illustrated for $[CpFe(CO)_2]_2^+$) are the 18-electron cationic species $[CpFe(CO)_2(NCCH_3)]^+$ and the 17-electron radical $CpFe(CO)_2^\bullet$. Subsequent reactions of the 17-electron radical species regenerate $[CpFe(CO)_2]_2$ and lesser amounts of $CpFe(CO)_2Cl$ via reaction with the solvent.

Acknowledgment. J.P.B. thanks the University of Minnesota Graduate School for a Stanwood Johnson Memorial Fellowship and the University of Minnesota Chemistry Department for a departmental fellowship sponsored by Shell. The FTIR spectrometer was purchased with funds from the NSF (Grant No. CHE 8509325). This work was funded in part by a grant from 3M.

Supplementary Material Available: Figures showing a cyclic voltammogram and an infrared spectroelectrochemical spectrum of $[Cp^*Fe(CO)_2]_2$, EPR spectra of $[CpFe(CO)_2]_2^+$ and $[Cp^*Fe(CO)_2]_2^+$, and kinetic plots of the reaction of $[Cp^*Fe(CO)_2]_2$ with acetonitrile (6 pages). Ordering information is given on any current masthead page.

Contribution from the Department of Chemistry, Auburn University, Auburn, Alabama 36849

Kinetic Behavior of Diazene in Aqueous Solution

David M. Stanbury

Received September 10, 1990

The acid-catalyzed hydrolysis of azodiformate ($(NCO_2)_2^{2-}$), which has diazene (N_2H_2) as an intermediate, has been studied by stopped-flow spectrophotometry. When the hydrolysis is conducted at sufficiently low pH (≈6), the second-order dismutation of diazene occurs on a time scale longer than that of its generation. The reduction of azobenzene-4,4′-disulfonate (ABDS) by diazene provides a convenient indicator of these reactions. The consumption of ABDS gives the relative rate constants of dismutation and reduction, and the kinetics study gives the absolute rate constants. At 25 °C these rate constants are 2.0×10^4 M^{-1} s^{-1} and 1.4×10^3 M^{-1} s^{-1}, respectively. A mechanism is proposed in which *cis*-diazene reduces ABDS and diazene competitively, both reactions proceeding by way of concerted dihydrogen transfer.

Introduction

Diazene, N_2H_2, also known as diimide, has a long history, dating back to the work of Thiele in 1892.[1] Presently, it is widely known as a cis-specific reducing agent,[2] although it has been implicated as an intermediate in numerous reactions[2] and may be important in nitrogen fixation[3] and atmospheric cloud chemistry.[4] Because of its simplicity and elusiveness it has been a subject of considerable theoretical interest.[5] Much of this interest has centered on its presumed mechanism of reduction, involving symmetry-allowed

(1) Thiele, J. *Liebigs Ann. Chem.* **1892**, *271*, 127–137.
(2) Back, R. A. *Rev. Chem. Intermed.* **1984**, *5*, 293–323.
(3) Hetterich, W.; Kisch, H. *Chem. Ber.* **1989**, *122*, 621–627.
(4) Costen, R. C.; Tennille, G. M.; Levine, J. S. *J. Geophys. Res.*, [*Atmos.*] **1988**, *93*, 15941–15954.
(5) Walch, S. P. *J. Chem. Phys.* **1989**, *91*, 389–394.

0020-1669/91/1330-1293$02.50/0